

## SIMULATION OF LASER DRILLING OF INCONEL X-750 AND TI-5AL-2.5SN SHEETS USING COMSOL

MUAMMEL M. HANON<sup>a,b,\*</sup>, ZIAD A. TAHA<sup>c</sup>, LÁSZLÓ ZSIDAI<sup>a</sup>

<sup>a</sup> MATE University, Szent István Campus, Mechanical Engineering Doctoral School, Páter Károly u. 1, 2100 Gödöllő, Hungary

<sup>b</sup> Middle Technical University (MTU), Baquba Technical Institute, Muasker Al Rashid Street, 10074 Baghdad, Iraq

<sup>c</sup> University of Baghdad, Institute of Laser for Postgraduate Studies, Industrial and Engineering Applications Department, Al-Jadriya, 10071 Baghdad, Iraq

\* corresponding author: [sharba.muammel.m.hanon@phd.uni-szie.hu](mailto:sharba.muammel.m.hanon@phd.uni-szie.hu)

**ABSTRACT.** This study aims to investigate the simulation of laser drilling processes on Inconel X-750 and Ti-5Al-2.5Sn sheets. To this end, COMSOL Multiphysics 5.2 software was employed to carry out the virtual experiments. A JK 701 pulsed Nd:YAG laser was used for drilling through the entire depth of Inconel X-750 and Ti-5Al-2.5Sn plates with a thickness of 2 mm and 3 mm, using laser pulses of a millisecond in time. The laser parameters varied in different combinations for well-controlled drilling through the entire thickness of the plates. Effects of laser peak power (10-20 kW) and pulse duration (0.5-2.5 ms) have been determined via studying the temperature distribution on the cross-section of the images taken in the simulation tests. Characterizing the optimum conditions obtained from the combination of parameters that improve the hole quality is an essential objective in this paper. The results suggest that the hole's diameter and depth have increased linearly as the laser beam's peak power and pulse duration are elevated. An improvement in the hole's taper ratio (the best value is 0.72) was observed as the laser beam pulse duration was longer, since an isosceles trapezoid shape was formed instead of a conical. The pulse duration exhibited more impact on the crater depth progression than the peak power. This work's outcomes might be helpful for researchers in terms of the optimum parameters proposed when studying the laser drilling of the mentioned alloys experimentally. The procedure and findings of this study are not presented elsewhere.

**KEYWORDS:** Laser drilling, modeling using COMSOL, Nd:YAG laser, Nickle alloys, Ti-5Al-2.5Sn alloy.

### 1. INTRODUCTION

Inconel X-750 is a high-strength, precipitation-hardenable Ni-Cr-Fe superalloy. Due to its oxidation and corrosion resistance and high strength at temperatures up to 704.5 °C, it is used in a wide range of applications such as forming tools, extrusion dies, test machine grips, and nuclear industry [1]. The alloy X-750 [2] has excellent properties down to cryogenic temperatures. These alloys are commonly employed in aerospace engineering, rotor blades and wheels of gas turbines as well [3].

Titanium and titanium alloys exhibit an excellent combination of mechanical and physical properties, coupled with low density (about half the weight of steel, copper, and nickel alloys) and exceptional corrosion resistance, which make them have a potential application in aerospace, industrial, automotive, biomedical, marine and railway industry [4–6]. Ti-5Al-2.5Sn alloy is characterized by weldability, non-ageability, and high strength; it offers high temperature stability, oxidation, and creep resistance. Therefore, it is used for the hot spots of the aerospace structural members, as in the case of areas that are close to engines [7].

Furthermore, it has, at cryogenic temperatures as low as -255 °C, an excellent fracture toughness [8].

Simultaneously, the laser is acquiring more importance owing to its possibility to be used for different machining and manufacturing processes, including but not limited to melting, drilling, cutting, cladding, alloying, and sintering [9, 10]. Among these techniques, laser drilling has become the novel technique for meeting a vast majority of possible industrial requirements for micro-hole drilling [11]. This technique is a thermal contact-free process, which involves shooting a number of successive focused pulses onto a target material [12]. The laser drilling process has several advantages over conventional techniques, such as accuracy, low heat input into the material, consistency and the ability to drill tiny holes with a diameter in the scale of microns facily [13]. Laser drilling is possible at different time scale regimes, including thermal or athermal mechanisms [14]. For the thermal mechanism, when continuous (CW) or long pulses are used, material removal occurs as a result of a conversion of the photon energy into thermal energy through the interaction of the intense electromagnetic waves in the laser radiation with the target material. Heating and melting occur with sufficient laser beam intensity;

vaporization occurs based on the material's temperature [15]. If the laser irradiance exceeds the threshold value, the drilling process is performed by evaporation [16]. The high density of the beam and excellent focusing characteristics of Nd:YAG lasers have made it suitable for drilling different materials [17]. There are many parameters related to the laser beam that affect the process of laser drilling, such as peak power, pulse duration, repetition rate, pulse shape, and focal plane position. These parameters should be optimized in order to obtain the desired hole quality. Taper angle, circularity, barrelling, and spatter formation are described as the features of a good-quality hole [18].

Many theoretical studies have been carried out to simulate laser drilling and determine the parameters that influence the application. Depending on the laser wavelength, energy and pulse width, the features of the hole will be determined. Verhoeven et al. referred that melting is one of several physical intermediate phenomena that have to be modelled in the simulation of the laser drilling process. Consequently, the simulation of melting profiles has been accomplished using both Stefan conditions and the physical quantity enthalpy models. Solving the problems of the enthalpy method was proven to be more efficient with multiple phases [19]. Salonitis et al. presented a theoretical model for simulating the process of laser drilling. They stated that the pulsing frequency of the laser beam has no effect if the maximum drill depth is achieved [20]. ANSYS FLUENT 6.3 package program has been employed to simulate the laser interaction with alumina ceramic plates by Hanon et al., where the effects of peak power and pulse width were studied. The parameters used in the experiments have been engaged for the drilling simulation. They have observed that the hole diameter increases when the peak power and pulse duration are increased [18]. Akhtar et al. developed a model on COMSOL package to simulate the ablation of nanosecond pulsed excimer laser in stainless steel and PMMA. Generating distorted edges with uneven surface is observed in the ablation process for steel, whereas in the case of PMMA, sharp edges were noticed. A higher efficiency of ablation has been reported with increasing the energy pulses for the case of steel, while the ablation of PMMA is found to be more efficient at low energy pulses [21].

In the present work, a COMSOL Multiphysics package has been used to simulate drilling a 3D geometry substrate irradiated by millisecond pulses of Nd:YAG laser beam. Nickel-base superalloys as well as titanium alloys became the desired choice for aerospace applications. For this, two different thicknesses of Inconel X-750 and Ti-5Al-2.5Sn alloys were examined by being subjected to laser irradiation. Two types of alloys were investigated to verify the simulation results, as the outcomes of two materials would confirm the observations better than one. Thus, the influence of varying laser beam parameters, type of material, and substrate thickness on the hole dimensions (pene-

Laser system specifications	Unit
Peak power	20 (kW)
Average power	230 (W)
Pulse width range	0.3-5 (ms)
Repetition rate range	5-150 (Hz)
Pulse energy	0.3-50 (J)
Laser wavelength	1064 ( $\mu\text{m}$ )

TABLE 1. Specifications of the laser system used in the simulations.

tration depth and diameters at inlet and outlet) has been assessed. The temperature distribution on the cross-sectional area along the drilled holes was performed.

## 2. COMSOL MODELING/INITIAL AND BOUNDARY CONDITIONS

The output of the JK 704 Nd:YAG laser system was appropriated as the heat source for simulating the laser drilling process in the present work. Table 1 shows the specifications of the laser system employed for this task. The pulse width is within millisecond range, as the energy of shorter pulse duration is not enough for the given task due to all the tests were conducted as a single shot (only one pulse).

Inconel X-750 and Ti-5Al-2.5Sn sheets with two different thicknesses (2 and 3 mm) were used during the present study for a laser drilling simulation by COMSOL Multiphysics 5.2 software. Selecting two different materials and thicknesses estimates the effect of the material type and thickness on drilled holes' quality. Several holes were carried out through a drilling simulation for each different material-thickness combination. The laser beam was focused on the substrates' top surface with a spot size of 240  $\mu\text{m}$  in diameter, and holes were drilled normal to the surface. Some laser beam parameters, such as peak power and pulse duration, have been changed systematically, while other laser beam parameters were kept constant. Table 2 shows the range of variation of laser beam parameters that were studied in the present work. All drilled holes were performed in the single-shot mode.

The procedure of assessing each parameter's influence was by changing just one parameter in every test while all other parameters were fixed. This way it is possible to better understand the drilled holes' progression in each laser beam parameter increment during the executed drilling process simulation.

The material substrate is a 3D geometry with the dimensions of 2 and 3 mm in thickness, 10 mm in length, and 10 mm in width. It was heated up by a laser beam fixed over the target's surface to produce the desired localized hole, as shown in Figure 1. The

Peak power	Pulse duration	Number of pulses	Focal plane position
10-20 kW, 2 kW increment	0.5-2.5 ms, 0.5 ms increment	Single Pulse	At surface

TABLE 2. Laser output parameters used in the drilling process simulation.

Property	Inconel X-750	Ti-5Al-2.5Sn	Unit
Density ( $\rho$ )	8.28	4.48	g/cm <sup>3</sup>
Thermal conductivity ( $k$ )	12	7.8	W/m. K
Specific heat capacity ( $C_p$ )	431	530	J/kg. K
Melting temperature (T)	1393-1424	1590 $\pm$ 20	$^{\circ}$ C
Vaporization temperature (T)	3150	3480	K
Emissivity ( $\epsilon$ ), oxidized surface at solid state	0.895	0.9	%
Emissivity ( $\epsilon$ ) at liquid state	0.925	0.7	%

TABLE 3. Thermo-physical properties of Inconel X-750 and Ti-5Al-2.5Sn alloys required for their drilling simulation [3, 22-24].

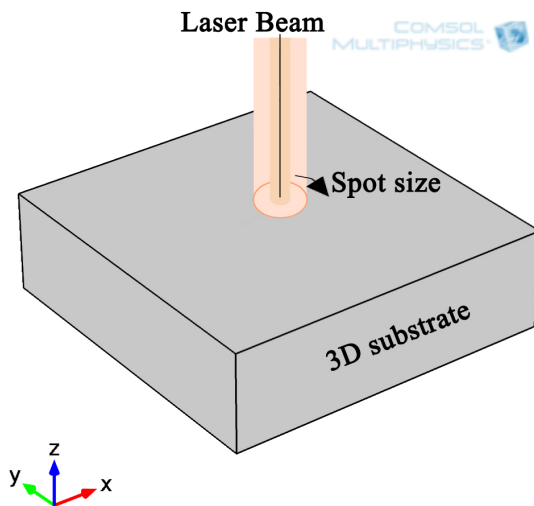


FIGURE 1. Laser beam irradiates a 3D substrate.

transient thermal response of the Inconel X-750 and Ti-5Al-2.5Sn sheets is obtained by modelling the incident heat flux gained from the laser beam as a heat source on the surface of specimens. The laser heat input at the laser beam spot centre has been assumed as a Gaussian profile with the maximum heat flux on the top surface. All other surfaces of the plate were assumed thermally isolated from the environment. This assumption is owing to the thermal equilibrium, as there is no heat transfer between the plate's surfaces and their contacts (surrounding) since they are the same temperature [25].

The substrate materials have been selected directly from the library of COMSOL Multiphysics 5.2 software. Therefore, the chemical composition of Inconel X-750 and Ti-5Al-2.5Sn alloys are already defined in the simulation program. The most important properties of the materials for this work's simulation purposes are listed in Table 3. It is noticed that the absorptivity

for Inconel X-750 alloy increases as the temperature rises while the opposite is true for the Ti-5Al-2.5Sn alloy.

Assuming isotropic thermal conductivity and neglecting the effect of convection, the heat is generated due to the high temperature of the laser beam heating. The governing heat conduction equation for the transient heat transfer module is given as follows [26].

$$\rho C_p \frac{\partial T}{\partial t} = k \nabla^2 T + Q \quad (1)$$

where  $\rho$  is the density of the workpiece material,  $C_p$  is the specific heat,  $k$  is the temperature-dependent thermal conductivity,  $Q$  is a distributed heat generation term and  $T$  is the temperature field as a function of space and time.

The laser power distribution varies within the laser spot from the maximum at the centre and vanishes toward the circumference. Accordingly, the heat flux input on the top surface of the workpiece is given by [27].

$$hf = \frac{2P}{\pi r_b^2} \frac{-2r^2}{r_b^2} \quad (2)$$

where  $hf$  is the laser heat flux,  $P$  is the laser power,  $r_b$  is the radius of the laser beam spot at the workpiece surface, and  $r$  is the radial distance from the laser beam spot centre.

According to Kirchhoff's law concerning thermal radiation in thermodynamic equilibrium, absorptivity and emissivity were assumed equal at the laser operating wavelength [28]. Based on that, the emissivity substituted absorptivity because the last was not given for the materials used. Thus, the heat load due to the laser is multiplied by the emissivity. The

energy balance at the drilling front can be expressed as [29]

$$q_0 = \varepsilon \cdot hf(x,y,t) \quad (3)$$

Also assuming that the laser is operating at a wavelength at which the workpiece material is opaque, no light is passing through it. Thus, all of the laser heat flux is deposited at the surface.

The workpiece material was generally meshed using a free triangular mesh. This meshing does not require a long time while processing but still preserves a reasonable element size in the thickness and plane. However, a finer mesh was applied for the laser beam spot area (the most crucial segment), as depicted in Figure 2a. This precise meshing would give slightly more accurate predictions for the peak temperature. The temperature distribution above the workpiece material is plotted in Figure 2b. The heating profile does introduce some significant temperature variations because the laser deposits a huge amount of heat. This heat sweeps the laser-beam incident area when it is focused at the top surface of the workpiece.

Image is taken from the workpiece's cross-section area seen in Figure 2c and 2d. It shows the temperature distribution on the workpiece material after a single laser pulse. The vaporized material is shown along the z-axis, where the laser beam penetrates the substrate depth. Inconel X-750 and Ti-5Al-2.5Sn alloys vaporized within 3150 and 3480 Kelvin, respectively. The white colour area shown in the figure represents the removed material that reaches a temperature higher than the vaporization temperature. The results also show the warm and cold sides next to the vertical line of the laser beam. Next to the ejected material, the warm side represents the heat-affected zone (HAZ) illustrated with gradient colours of the temperature distribution.

The model examines the influence of the laser beam power and pulse width on the geometry of the drilled holes (depth and diameters of inlet and outlet). The temperature variations across the material substrate are computed during the heating process.

### 3. RESULTS AND DISCUSSION

Effects of laser peak power and pulse duration vs. hole diameters (Inlet and Outlet) and depth are the most critical aspects of this study. As mentioned in Table 3, Inconel X-750 and Ti-5Al-2.5Sn alloys were experimentally observed to vaporize at 3150 and 3480 K, respectively. Therefore, the vaporization temperature was adopted for the used materials in the present work within this range. Thus, the removed material represented by the white colour area indicates that it reached to/higher-than the vaporization temperature.

To determine the influence of the laser peak power on the hole dimensions, the laser beam was focused onto the Inconel X-750 alloy specimen's surface with

different powers (ranged between 10 and 20 kW, with an increment of 2 kW) and at a constant pulse duration of 1 ms where the plate's thickness was 2 mm, as shown in Figure 3 ((a)-(f) top left). It can clearly be seen that the hole diameters and depths increased as the laser beam's peak power increased. Although the crater was blind (the drilling had not reached a full hole) until 18 kW, the hole's depth heightened as the peak power raised. At 20 kW, the full hole was achieved where an outlet hole was created. This is in good agreement with a published study that showed the keyhole depth is almost linearly increased with the rise of power density [30]. They attributed this to the relatively long time of interaction between the laser and the material as well as the intense thermal effect. Thus, it is facile to produce a deep hole in the mm scale. This would also confirm another study's simulation and experimental outcomes concerning the laser drilling of alumina by employing the ANSYS FLUENT model [18]. The authors found out that the hole's depth and diameter have increased by adjusting (increasing) the pulse width and peak power when applying a single pulse.

The impact of the pulse duration was also examined on the same Inconel X-750 alloy plate whose thickness was 2 mm, by employing various pulse durations within 0.5 to 2.5 ms at a fixed peak power of 15 kW, as exhibited in Figure 3 ((a)-(f) top right). Here, the full hole was reached at a pulse duration of 1.5 ms. The taper ratio is the ratio of the hole outlet to the hole inlet in terms of diameter. This ratio becomes better when its value approaches 1, which means that the hole inlet and outlet diameter are almost equivalent. It was noticed that the taper ratio at 1.5 ms pulse duration was 0.37, whereas it reached 0.63 at a pulse duration of 2.5 ms. Hence, this indicates an improvement in the taper ratio as the pulse duration was longer. The morphology of a keyhole drilled with a laser in different pulse duration ranged between 0.5-2.5 ms (with an increment of 0.5 ms) was evaluated [30]. The researchers stated that a shorter pulsed laser obtained better keyhole quality. A smooth keyhole wall could be formed with a pulse duration of less than 1 ms, while a valley-and-peak structure appeared with a longer than 1 ms pulse duration.

The same process parameters (conditions) were used to simulate the laser drilling of Ti-5Al-2.5Sn alloy at a plate thickness of 2 mm with variable peak power and pulse duration as displayed in Figure 3 (bottom left and bottom right), respectively. When the peak power varied (from 10 to 20 kW), the pulse duration kept constant at 1 ms. Nevertheless, the peak power was fixed at 15 kW while the pulse duration was changed (from 0.5 to 2.5 ms). The full hole was achieved at 14 kW when varying the peak power. When the pulse duration is the variable parameter, a full hole was achieved at 1 ms. This points out that laser drilling of Ti-5Al-2.5Sn alloy could be carried out with lower

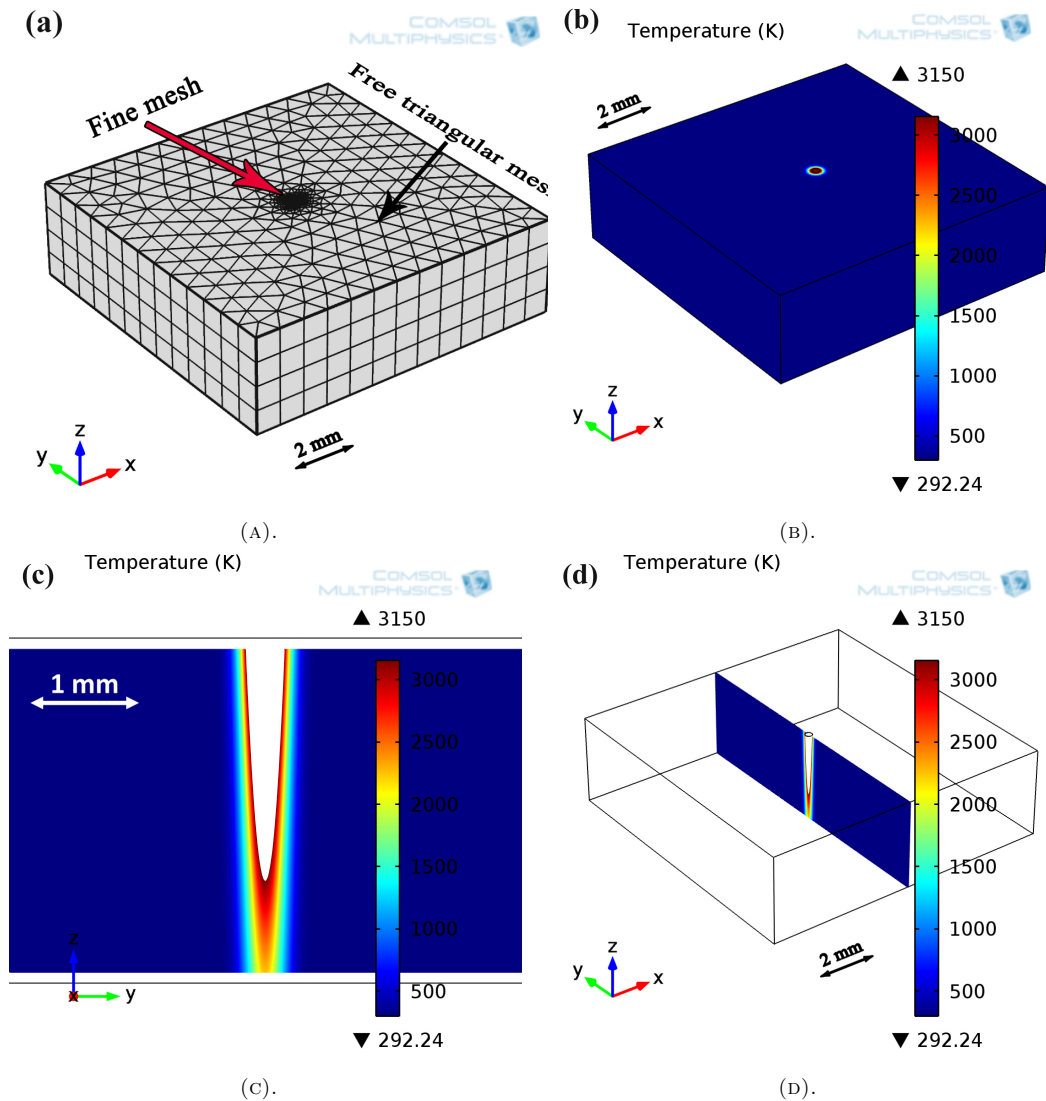


FIGURE 2. (a) A 3D mesh of the substrate, refined along the laser spot area, (b) temperature distribution at the substrate surface after the laser drilling process, (c) 2D front view for temperature distribution on the cross-section along with the hole, and (d) a slice is taken from 3D view.

power and shorter time as compared to the Inconel X-750 alloy when using the same process conditions.

To summarize the tested parameters' effect, a comparison between the obtained dimensions (inlet and outlet diameters) for both the Ti-5Al-2.5Sn and the Inconel X-750 alloys versus peak power and pulse duration presented in Figures 4 and 5, respectively. It is obvious that diameters achieved for hole inlet and outlet of Ti-5Al-2.5Sn were always larger than in the case of the Inconel X-750 alloy at the same conditions employed. This might be ascribed to the difference in the thermal conductivity of the materials used. According to the heat diffusion equation, the higher the thermal conductivity, the greater the heat dissipation rate [31], resulting in less impact in the area struck by the laser due to not storing thermal energy. Thus, these outcomes were expected since the Ti-5Al-2.5Sn has a lower thermal conductivity than the Inconel X-750 alloy. The diameter value of the

hole outlet never reached a diameter value near the inlet, making the taper ratio, in general, inferior. The best taper ratio value (0.72) was observed for the laser drilling of Ti-5Al-2.5Sn alloy at process parameters of 15 kW peak power and 2.5 ms pulse duration, where an isosceles trapezoid shape of the hole was formed instead of a conical shape. A full crater penetration in the Inconel X-750 alloy was scarcely accomplished, as the hole was blind (without an outlet) in most cases. This indicates that crater diameters (inlet and outlet) and depth could be controlled by governing the drilling process's laser peak power and pulse duration.

Figures 6 and 7 illustrate the diameters (inlet and outlet) of Ti-5Al-2.5Sn and Inconel X-750 alloys with a plate thickness of 3 mm versus the peak power and pulse duration, respectively. This was carried out to investigate the effect of utilizing a thicker plate when simulating the employed alloys' laser drilling. A similar tendency was observed regarding the taper

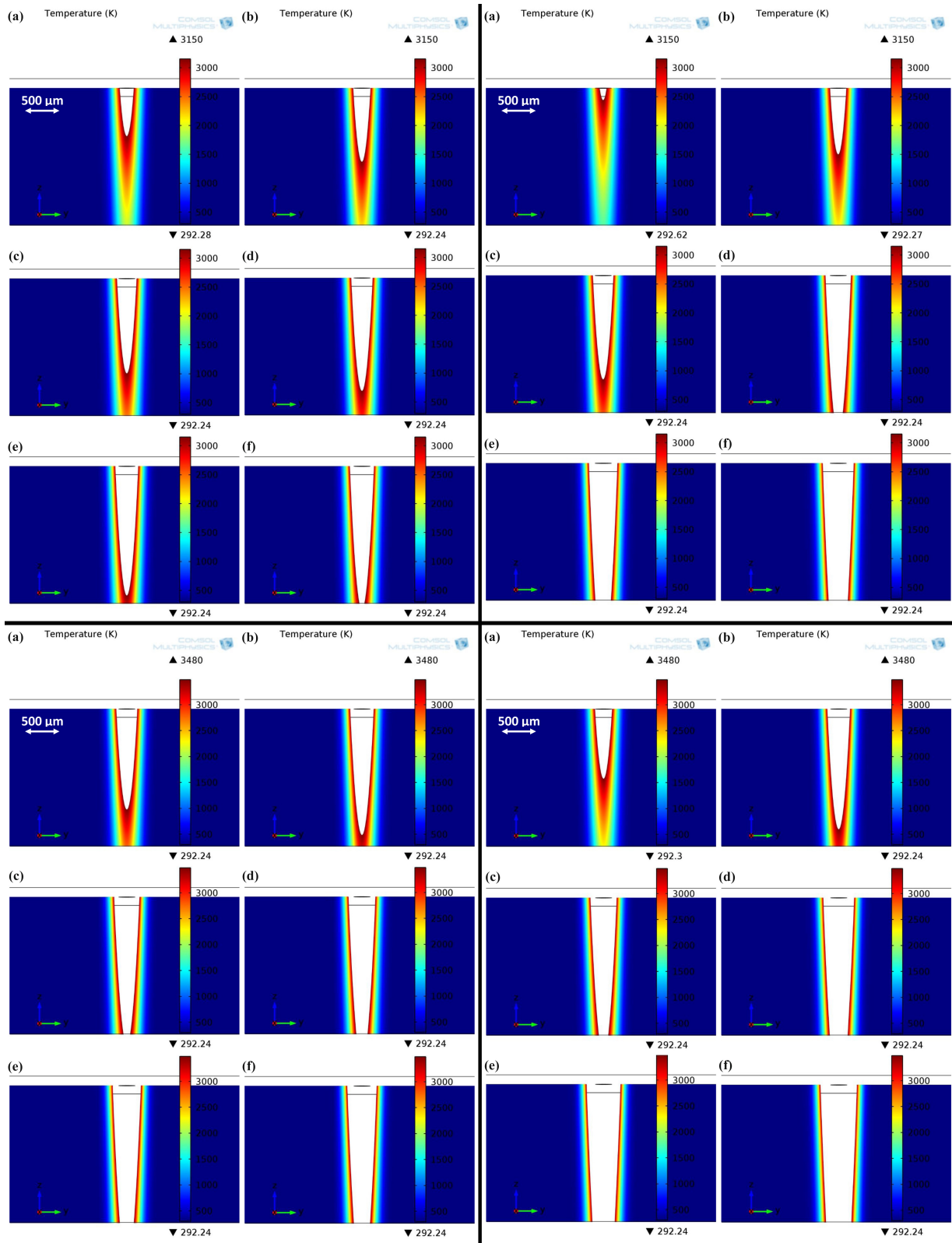


FIGURE 3. Laser drilling of 2 mm thick metal plates: at 1ms pulse duration and peak power of (a) 10, (b) 12, (c) 14, (d) 16, (e) 18, and (f) 20 kW for Inconel X-750 alloy plate (top left) and Ti-5Al-2.5Sn alloy (bottom left); at 15 kW peak power and pulse duration of (a) 0.5, (b) 0.75, (c) 1, (d) 1.5, (e) 2, and (f) 2.5 ms for Inconel X-750 alloy (top right) and Ti-5Al-2.5Sn alloy (bottom right). The scale is the same in all figures.

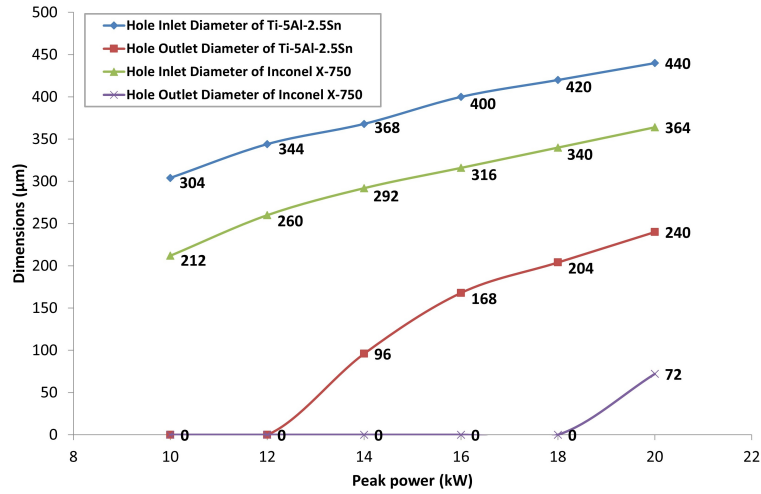


FIGURE 4. Peak power versus diameters (inlet and outlet) for the thickness of 2 mm, 1 ms pulse duration, and various peak powers.

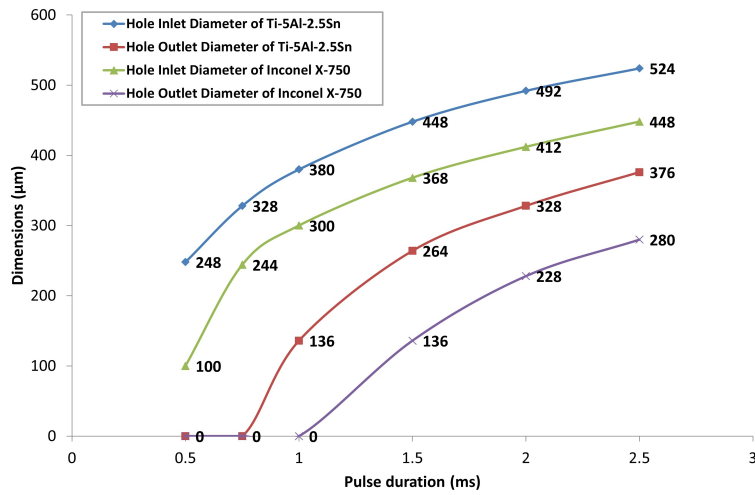


FIGURE 5. Pulse duration versus diameters (inlet and outlet) for the thickness of 2 mm, 15 kW peak power, and various pulse durations.

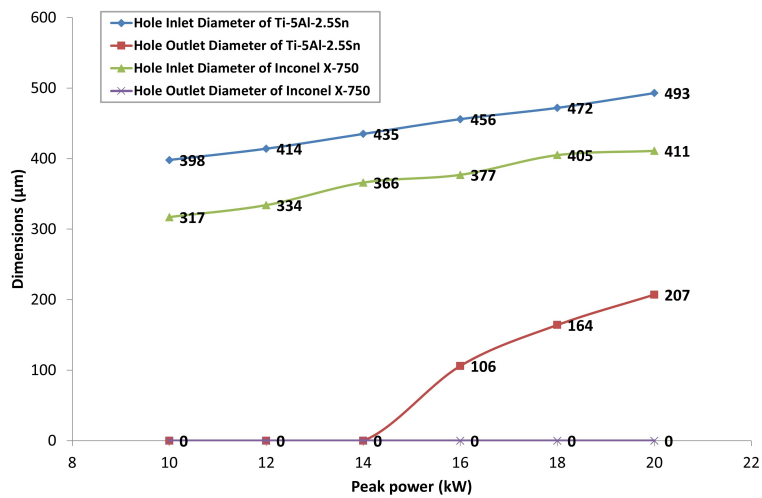


FIGURE 6. Peak power versus diameters (inlet and outlet) for the thickness of 3 mm, 1.5 ms pulse duration, and various peak powers.

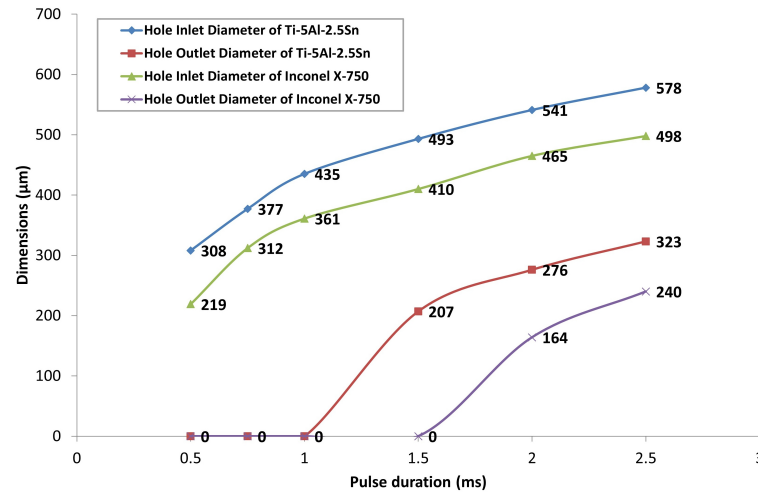


FIGURE 7. Pulse duration versus diameters (inlet and outlet) for the thickness of 3 mm, 20 kW peak power, and various pulse durations.

ratio compared to the sheets of 2 mm in thickness. The best taper ratio value (0.56) was also achieved for the Ti-5Al-2.5Sn alloy at a peak power of 15 kW and a pulse duration of 2.5 ms. Simultaneously, a failure in piercing a whole crater was revealed in numerous test conditions and mainly in the case of the Inconel X-750 alloy, where the full hole was not reached at less than 20 kW peak power and 2 ms pulse duration. This resulted in reducing the hole's taper of the specimens at this thickness (3 mm) as compared to the thinner ones (2 mm). A similar behaviour was observed in micro-holes drilled utilizing pulsed Nd:YAG laser on a nickel-based superalloy [32] as the minimal taper was observed in the case of the thicker sample (4.5 mm). At the same time, the maximum was observed in the case of the smaller thickness (0.5 mm).

Figures 8 and 9 demonstrate the hole depth formation's progression versus the peak power and pulse duration, respectively. Both used alloys (Ti-5Al-2.5Sn and Inconel X-750) of 2 and 3 mm thicknesses were represented in these two figures to be compared. It can clearly be seen that the hole depth increases with increasing peak power and pulse duration in all cases. The crater opened from the outlet side in a shorter pulse time (1 ms) and less power (14 kW) for Ti-5Al-2.5Sn alloy as compared to the Inconel X-750 alloy (1.5 ms and 15 kW). This can be attributed to the lower thermal conductivity of the Ti-5Al-2.5Sn alloy, as low thermal conductivity benefits retaining the heat in a restricted zone and limits the development of heat dissipation. Investigating both Figures 8 and 9 shows that the pulse duration as a parameter in the laser drilling process exhibited more impact on the crater depth than the peak power. Considering that change in the pulse duration parameter was more effective in the progression to create an entire hole. This would agree with the outcomes of a published study about modelling and optimizing the geometrical features (circularity and taper of the hole at entrance and exit)

of laser trepan drilled holes in Ti-6Al-4V alloy. The results showed that the pulse width is a significant factor for hole taper and hole circularity [33].

#### 4. CONCLUSIONS

COMSOL software was employed to simulate the laser drilling process of Inconel X-750 and Ti-5Al-2.5Sn alloys in the form of sheets for the thicknesses of 2 and 3 mm utilizing a pulsed Nd:YAG laser. This study was carried out to determine the influence of laser drilling process parameters, such as peak power (ranged between 10 and 20 kW with an increment of 2 kW) and pulse duration (extended within 0.5 to 2.5 ms with an increment of 0.5 ms), on the hole dimensions (hole inlet and outlet diameters and hole depth) of the used materials. Based on the observations of the results, the following conclusions can be drawn:

- The diameter and depth of the hole have increased linearly as the laser beam's peak power and pulse duration increased, observing a considerable difference between the hole entrance and the exit diameter.
- An improvement in the taper ratio was observed as the laser beam pulse duration was longer. The best taper ratio value (0.72) was observed at 2.5 ms pulse width.
- The material properties showed an impact on the holes drilled by laser. The crater of the Ti-5Al-2.5Sn substrate opened from the outlet side at a shorter pulse duration and less power due to the lower thermal conductivity, which benefits from retaining the heat in a restricted zone and limiting heat dissipation development.
- The hole's shape can be enhanced when employing a particular combination of laser beam parameters. An isosceles trapezoid shape of the crater was formed instead of a conical while drilling the Ti-5Al-2.5Sn alloy (2 mm in thickness) at 15 kW peak power and 2.5 ms pulse duration.

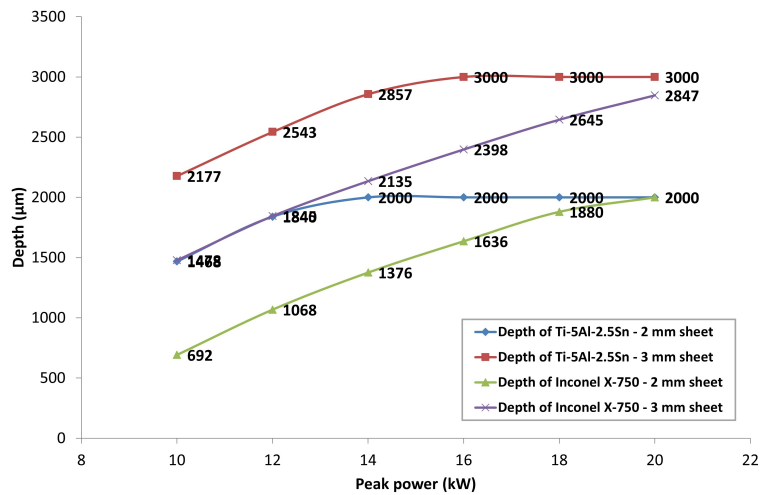


FIGURE 8. Hole depth versus different peak power, at 1 ms pulse duration when thickness is 2 mm; and at 1.5 ms pulse duration when thickness is 3 mm.

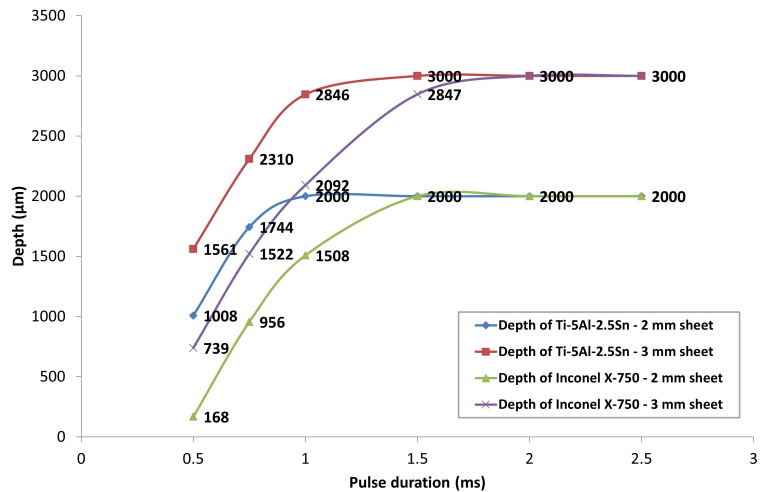


FIGURE 9. Hole depth versus different pulse durations, at 15 kW peak power when thickness is 2 mm; and at 20 kW peak power when thickness is 3 mm.

- The thickness of the specimens has a significant influence on developing a complete hole. For the same used material, a failure in piercing a full crater (the holes remained blind) in numerous test conditions was noticed when drilling the specimens of 3 mm in thickness. In contrast, opened holes were achieved in much shorter pulse times and lower power for the pieces with a thickness of 2 mm.
- As a parameter in the laser drilling process, pulse duration exhibited more impact on the crater depth progression than the peak power, as varying the pulse duration was more effective for producing a perfect hole.

ACKNOWLEDGEMENTS

This work was carried out at the labs of the Institute of Laser for Postgraduate Studies at the University of Baghdad, Iraq. The authors gratefully acknowledge Prof. A Hadi Janabi, the dean of the institute at that time, to permit us to use the institute licensed package of COMSOL Multiphysics v 5.2.

REFERENCES

- [1] K. Fisher, et al. Multi scale characterization of stress corrosion cracking of alloy X750. *MRS Online Proceedings Library* **1519**(1002), 2013. <https://doi.org/10.1557/opl.2012.1761>.
- [2] A. Tazehkandi, et al. Experimental investigations of cutting parameters' influence on cutting forces and surface roughness in turning of inconel alloy X-750 with biodegradable vegetable oil. *Proceedings of the Institution of Mechanical Engineers, Part B: Journal of Engineering Manufacture* **231**(9):1516–1527, 2017. <https://doi.org/10.1177/0954405415599914>.
- [3] K. Sabareesaan, et al. Analysis of the effect of process parameters in electric discharge machining of inconel X750 using brass electrode. *International Journal of Engineering Research & Technology* **3**(9):1180–1184, 2014.
- [4] C. Bandapalli, et al. High speed machining of ti-alloys-A critical review. In *1st International and 16th*

- National Conference on Machines and Mechanisms, iNaCoMM 2013*, pp. 324–331, 2013.
- [5] N. Al-Mobarak, et al. Corrosion behavior of Ti-6Al-7Nb alloy in biological solution for dentistry applications. *International Journal of Electrochemical Science* **6**(6):2031–2042, 2011.
- [6] J. Krčil, et al. The characterization of anodic oxide layers on selected bio-compatible titanium alloys. *Acta Polytechnica* **58**(4):240–244, 2018. <https://doi.org/10.14311/AP.2018.58.0240>.
- [7] B. Zhang, et al. Strain-rate-dependent tensile response of Ti-5Al-2.5Sn alloy. *Materials* **12**(4):659, 2019. <https://doi.org/10.3390/ma12040659>.
- [8] K. Wei, et al. Selective laser melting of Ti-5Al-2.5Sn alloy with isotropic tensile properties: The combined effect of densification state, microstructural morphology, and crystallographic orientation characteristics. *Journal of Materials Processing Technology* **271**:368–376, 2019. <https://doi.org/10.1016/j.jmatprotec.2019.04.003>.
- [9] T. Kozior. The influence of selected selective laser sintering technology process parameters on stress relaxation, mass of models, and their surface texture quality. *3D Printing and Additive Manufacturing* **7**(3):126–138, 2020. <https://doi.org/10.1089/3dp.2019.0036>.
- [10] T. Kozior, et al. Waviness of freeform surface characterizations from austenitic stainless steel (316L) manufactured by 3D Printing-Selective Laser Melting (SLM) technology. *Materials* **13**(19):4372, 2020. <https://doi.org/10.3390/ma13194372>.
- [11] Q. Zhang, et al. A study on film hole drilling of IN718 superalloy via laser machining combined with high temperature chemical etching. *The International Journal of Advanced Manufacturing Technology* **106**:155–162, 2020. <https://doi.org/10.1007/s00170-019-04541-0>.
- [12] K. Aljanabi. Effect of high energy nd:glass laser on the drilled in the 5052 Al-Mg alloy. *Iraqi Journal of Laser* **18**(2):35–40, 2019.
- [13] J. Collins, P. Gremaud. A simple model for laser drilling. *Mathematics and Computers in Simulation* **81**(8):1541–1552, 2011. <https://doi.org/10.1016/j.matcom.2010.07.010>.
- [14] Fundamentals of laser-material interaction and application to multiscale surface modification. In *Laser Precision Microfabrication*, pp. 91–120, 2010. [https://doi.org/10.1007/978-3-642-10523-4\\_4](https://doi.org/10.1007/978-3-642-10523-4_4).
- [15] M. Hasan, et al. A review of modern advancements in micro drilling techniques. *Journal of Manufacturing Processes* **29**:343–375, 2017. <https://doi.org/10.1016/j.jmapro.2017.08.006>.
- [16] Z. Taha. Hole drilling of high density polyethylene using Nd:YAG pulsed laser. *Iraqi Journal of Laser* **18**(1):7–12, 2019.
- [17] A. Samant, et al. Computational approach to photonic drilling of silicon carbide. *The International Journal of Advanced Manufacturing Technology* **45**:704–713, 2009. <https://doi.org/10.1007/s00170-009-2004-0>.
- [18] M. Hanon, et al. Experimental and theoretical investigation of the drilling of alumina ceramic using Nd:YAG pulsed laser. *Optics & Laser Technology* **44**(4):913–922, 2012. <https://doi.org/10.1016/j.optlastec.2011.11.010>.
- [19] J. Verhoeven, et al. Modelling laser induced melting. *Mathematical and Computer Modelling* **37**(3-4):419–437, 2003. [https://doi.org/10.1016/S0895-7177\(03\)00017-7](https://doi.org/10.1016/S0895-7177(03)00017-7).
- [20] K. Salontis, et al. A theoretical and experimental investigation on limitations of pulsed laser drilling. *Journal of Materials Processing Technology* **183**(1):96–103, 2007. <https://doi.org/10.1016/j.jmatprotec.2006.09.031>.
- [21] S. Akhtar, et al. Simulations and experiments on excimer laser micromachining of metal and polymer. *Journal of Micro/Nanolithography, MEMS, and MOEMS* **13**(1):013008, 2014. <https://doi.org/10.1117/1.JMM.13.1.013008>.
- [22] Special metals corporation: INCONEL alloy X-750, 2004.
- [23] M. Khan, M. Rahman. Surface characteristics of Ti-5Al-2.5Sn in electrical discharge machining using negative polarity of electrode. *The International Journal of Advanced Manufacturing Technology* **92**:1–13, 2017. <https://doi.org/10.1007/s00170-017-0028-4>.
- [24] K. Wei, et al. Preliminary investigation on selective laser melting of Ti-5Al-2.5Sn  $\alpha$ -Ti alloy: From single tracks to bulk 3D components. *Journal of Materials Processing Technology* **244**:73–85, 2017. <https://doi.org/10.1016/j.jmatprotec.2017.01.032>.
- [25] H. Qian. The zeroth law of thermodynamics and volume-preserving conservative system in equilibrium with stochastic damping. *Physics Letters A* **378**(7-8):609–616, 2014. <https://doi.org/10.1016/j.physleta.2013.12.028>.
- [26] W. Han. *Computational and experimental investigations of laser drilling and welding for microelectronic packaging*. Worcester Polytechnic Institute, Ma, USA, 2004.
- [27] O. Abdulghani, et al. Modeling and simulation of laser assisted turning of hard steels. *Modeling and Numerical Simulation of Material Science* **3**(4):106–113, 2013. <https://doi.org/10.4236/mnsms.2013.34014>.
- [28] J. Deng, et al. The influence of wavelength-dependent absorption and temperature gradients on temperature determination in laser-heated diamond-anvil cells. *Journal of Applied Physics* **121**(2):025901, 2017. <https://doi.org/10.1063/1.4973344>.
- [29] S. Marinetti, P. Cesaratto. Emissivity estimation for accurate quantitative thermography. *NDT & E International* **51**:127–134, 2012. <https://doi.org/10.1016/j.ndteint.2012.06.001>.
- [30] Y. Zhang, et al. Modeling and simulation on long pulse laser drilling processing. *International Journal of Heat and Mass Transfer* **73**:429–437, 2014. <https://doi.org/10.1016/j.ijheatmasstransfer.2014.02.037>.
- [31] D. Zhao, et al. Measurement techniques for thermal conductivity and interfacial thermal conductance of bulk and thin film materials. *Journal of Electronic Packaging* **138**(4):040802, 2016. <https://doi.org/10.1115/1.4034605>.

[32] M. Gurav, et al. Quality evaluation of precision micro holes drilled using pulsed Nd:YAG laser on aerospace nickel-based superalloy. *Materials Today: Proceedings* **19**(2):575–582, 2019.  
<https://doi.org/10.1016/j.matpr.2019.07.736>.

[33] R. Goyal, A. Dubey. Modeling and optimization of geometrical characteristics in laser trepan drilling of titanium alloy. *Journal of Mechanical Science and Technology* **30**:1281–1293, 2016.  
<https://doi.org/10.1007/s12206-016-0233-3>.